Adaptive Calibration of Diesel Engine Injection for Minimising Fuel Consumption with Constrained $\mathrm{NO_x}$ Emissions in Actual Driving Missions

José Manuel Luján[1] , Benjamín Pla [1], Pau Bares [1], Varun Pandey [1]

Abstract

This paper proposes a method for fuel minimisation of a Diesel engine with constrained $\mathrm{NO_x}$ emission in actual driving mission. Specifically, the methodology involves three developments: The first is a driving cycle prediction tool which is based on the space-variant transition probability matrix obtained from an actual vehicle speed dataset. Then, a vehicle and an engine model is developed to predict the engine performance depending on the calibration for the estimated driving cycle. Finally, a controller is proposed which adapts the start-of-injection calibration map to fulfill the $\mathrm{NO_x}$ emission constraint while minimising the fuel consumption. The calibration is adapted during a pre-defined time window based on the predicted engine performance on the estimated cycle and the difference between the actual and the constraint on engine $\mathrm{NO_x}$ emissions. The method assessment was done experimentally in the engine test setup. The engine performace using the method is compared with the state-of-the-art static calibration method for different $\mathrm{NO_x}$ emission limits on real driving cycles. The online implementation of the method shows that the fuel consumption can be reduced by 3-4 % while staying within the emission limits, indicating that the estimation method is able to capture the main driving cycle characterstics.

Keywords

Diesel engine online calibration; Adaptive calibration; Fuel consumption minimisation; Constrained $\mathrm{NO_x}$ emissions; Online optimisation

Introduction

Motivated by the requirement of improvement in fuel-efficiency with minimal emissions, the control of Diesel-engine is being investigated by many researchers[1]. Diesel-based vehicles are largely responsible for the $\mathrm{NO_x}$ emissions according to Hooftman et. al in[2]. Despite the continuous tightening of the $\mathrm{NO_x}$ type approval limits from EU1 to EU6, Chen et. al[3] highlight that the difference between the type approval $\mathrm{NO_x}$ and the real world $\mathrm{NO_x}$ emissions has grown over the years. The reason for this discrepancy is the uncertainty due to driving dynamics, ambient temperature and road sloap during real driving conditions which are not considered in the engine optimisation process. State-of-the-art engine optimisation method is based on feedback and feedforward controllers. Fixed look-up tables are employed as the set-point generator and feedforward controller. The maps are obtained during the calibration process as shown by the authors in[4,5] with a goal of minimising fuel consumption with regulatory constraint on emissions on a predefined homologation cycle. The fact that the fixed calibrations are used regardless of the driving condition causes the engine not to operate in an optimal way during real driving. A high level of control is required in the engine for it to run optimally in the real driving condition. To this aim the controller is required to have three main features:

- Vehicle speed prediction model is required to assess the uncertainities in the real world scenario and it can be based on the available information about vehicle speed on a given route. One option is to model the vehicle speed using Markov chains, as described by the authors in[6]. This includes extracting information from a database of real world driving and to generate the driving cycle using a stochastic process.
- A vehicle model is necessary for the online estimation of the engine performance. Although, some works have applied Optimal Control to vehicle powertrains without the so called quasi-static engine simplifications[7], very simplistic 0D models should be applied for online purpose. For this reason, the present paper considers the quasi-static engine approximation previously followed in other works[8–10]. In the article by Yang et al.[11], start-of-injection is shown to control the engine tradeoff performance between fuel consumption and $\mathrm{NO_x}$ emissions.
- A supervisory controller is required to optimally control the engine for minimised fuel consumption with constrained emissions. Optimal control theory has been widely used in literature as consolidated by

[1]CMT–Motores Térmicos, Universitat Politècnica de València, Valencia, Spain

Corresponding author:
Varun Pandey, CMT–Motores Térmicos, Universitat Politècnica de València, Camino de Vera Sn, E-46022 Valencia, Spain
Email: vapan2@mot.upv.es

the authors in[12] to address complex control problem. However application of these methods in engine management system is still a big challenge due to their computational cost. Some other methods have been focused on lower level engine control for Spark-Ignition Engine. Extremum seeking method has been widely used in[13–16], most of the work is related to online optimal calibration but does not inlcude real driving emission constraint. The authors in[17], present a theoritical basis and algorithmic implementation for allowing the engine to learn the optimal set values of accesible variables in real-time, while running a vehicle. Even though short transients have been presented for online optimisation, the applicability of this method in real driving condition still remains an unsolved issue. Other methods, like Equivalent Consumption Minimisation Strategy (ECMS) and Model Predictive Control (MPC) as in[18,19], seem to be more promising in solving the issues of real-time control of Diesel engine. Stephan et. al[20] propose an ECMS method to provide a solution for online optimal control of Diesel engine with constraint in $\mathrm{NO_x}$ emission. The authors assume a constant emission reference target resulting in unrealistic emission during real driving conditions. In the article by Gokul et.al[21], MPC is formulated to maximise the fuel efficiency while tracking boost pressure and exhaust gas recirculation rate references, in the face of uncertainties, adhering to the input, safety constraints and constraints on emissions averaged over some finite time period. Authors in[22], present a model based approach to the adaption of the engine calibration to the driver behaviour and the target pollutant emissions: they consider a fixed probability matrix for expected engine operating points, which does not represent a real world scenario.

This paper proposes a look-ahead based methodology to continually adapt the engine calibration such that the fuel consumption is minimised while fulfilling the $\mathrm{NO_x}$ emission constraint in real driving condition. The strategy is to estimate the vehicle speed using the Markov chain model and then calculate the fuel consumption and the $\mathrm{NO_x}$ emission for a time window using a 0D vehicle model. The calculation is done with different sets of start-of-injection (SOI) calibration and at the end of every time window there exist a set of SOI maps associated with different levels of cumulative fuel consumption and emissions. A supervisory controller updates the calibration from the available set such that, fuel consumption is minimised while $\mathrm{NO_x}$ emission is less than the limit in the upcoming time window. The constraint on $\mathrm{NO_x}$ emission is time dependent and is calculated as the difference between the actual $\mathrm{NO_x}$ emission (measured by the sensor) and the $\mathrm{NO_x}$ emission limit.

Further, the article is structured as follows: Next section describes the problem and its proposed solution, The developed tools have been described in the order of vehicle speed prediction method, vehicle model and the proposed control method has been elaborated followed by the experimental setup. Finally, the results of the case study are presented followed by conclusion and the summary.

Problem description

The standard engine calibration approach consists on taking a driving cycle, e.g. the New European Driving Cycle (NEDC), or a set of them to make an optimisation and then use the obtained results to fill the calibration maps. However, in this case, the optimality of the calibration for a given driver will depend on the similarity between the NEDC and his driving patterns. Moreover, this approach neglects other boundaries as the traffic, pollution levels in the area or other environmental conditions. On the other hand, optimal control approach require a priori knowledge of the driving cycle, which prevents its application for real-time control. To overcome these drawbacks, as an intermediate solution between the optimal control approach and the static calibration approach, the present paper poses the calibration problem as finding a set of optimal calibration maps containing the set points that minimise the accumulated fuel consumption $(\mathrm{m_f})$ over a sequence of engine speeds and torques $(\mathrm{n_e}, \mathrm{M_d})$ representative of the driving conditions for a driver, while fulfilling constraints on emissions for unknown driving conditions.

Adaptive Calibration based on Power Demand Estimation

Application of engine controls in real driving conditions for minimising fuel consumption with constrained emissions requires vehicle speed prediction model which could also account for the real driving uncertainities, simple but accurate engine and vehicle model to estimate engine performace and finally a controller to calculate and implement optimal actuations. The trip could be discretised in space, where each section is called window and based on the predicted emissions for an upcoming window, the control actions that minimise fuel consumption keeping emissions within certain limits, could be calculated and stored as calibration maps, that could be applied during the next time window. In this sense, the proposed control algorithm has three layers: The first one is the estimation of power demands in a predicting horizon, the second one computes the expected fuel consumption and $\mathrm{NO_x}$ emissions depending on the SOI calibration used (from a limited set of possible calibrations). The last phase applies the calibration with minimum expected fuel consumption from those whose expected $\mathrm{NO_x}$ emissions are below a predefined limit.

In Figure 1, schematic of the high level control system of the developed method is presented. where v_{estim} and v_{real} are the estimated and actual vehicle speeds respectively. Prediction horizon window (PHW) is the moving time window for which the fuel consumption and engine out $\mathrm{NO_x}$ emissions are cumulated. The length of the PHW is a design choice (calibration parameter) which affects the closeness of the cumulative NOx emissions at the end of the cycle from the target emissions/limits. Larger the window, farther will be the NOx emissions from the target. On the contrary, short windows will avoid fuel reduction potential since the problem will be transformed on tracking a constant NOx emission, and will have an excessive computation cost for the real-time implementation. For the purpose of explanation, the schematic has three time frames represented by the three columns as past, present and upcoming time windows. During each PHW there are three processes happening in parallel, represented by the three rows. The top row represents the first process, which is regarding the *estimation* of driving cycle and calculation of engine speed and torque from vehicle speed demand. The second process as in central row is regarding the *calculation* of the control actions and their conversion into the calibration maps. Finally, bottom row represents the third process which is regarding the *application* of the stored calibration maps, calculated during the previous PHW. The calculation of the optimal calibration map is based on the predicted NO_x emissions for the upcoming PHW, the measured NO_x emission in the previous PHW and the NO_x emission limit. At the end of PHW, the calibration is adapted in order minimise fuel consumption while keeping NO_x emission under a certain limit. In this study, PHW (in red boxes) is chosen to be 100 sec. It must be noticed that during the first time window, standard calibration map is applied. Further, each subsystem is described in the following subsections.

Vehicle speed prediction model

The vehicle speed prediction process uses Markov chain due to its relative simplicity in representing an unknown system. Markov property means that the future states depend only on the present states and are independent of the past states. Let the state $x_n = v_n$ where v_n is the current vehicle velocity. A Markov chain is a sequence of random variables X_1,X_2, ...X_n whose conditional probabilities are expressed as;

$$\begin{aligned} P(X_{n+1} = x_{n+1} | X_1 = x_1, X_2 = x_2, \ldots, X_n = x_n) \\ = P(X_{n+1} = x_{n+1} | X_n = x_n) \end{aligned} \quad (1)$$

The set of possible values that the random variables X_n can take is called the state space of the chain. The conditional probabilities are called transition probabilities. The sum of all probabilities leaving a state must satisfy:

$$\sum_j p_{ij} = \sum_j P(X_{n+1} = j | X_n = i) = 1 \quad (2)$$

p_{ij} is predicted by all the transitions that have occurred in the previously recorded driving cycle, on the same route. The probability used in the synthesis procedure is space dependent, that is, as the vehicle moves on, the probability of evolving from one state (vehicle velocity) to another may change. In other words, the controller requires two parameters to make a prediction of vehicle velocity: first it needs the current position of the vehicle which determine the transition probability matrix to be applied and then it requires the knowledge of the velocity in the previous time step to determine the probability distribution of the current state and hence the prediction is made.

Transition probabilities are stored as Transition Probability Matrix for thirty equally divided sections (s) of the route (approximately 60 km). In the present work the vehicle speed is the system state ($x_n = v_n$) and its sequence in each section of the route is used to build the Transition Probability Matrices. For practical reasons, the data has been discretised in steps of 1 km/h in velocity. The process of cycle synthesis could be summarised as :

Step 1: Transition probability matrices (TPM_s), where s represents the section from which the tranistion probabilities have been extracted from the experimental data for the route under consideration. In particular, the probabilities are assumed to be equal to the event frequency during a given section.

Step 2: The inputs to the generator are the initial vehicle velocity (v_0), vehicle position or the section of route (s) and the Cumulative Probability Function derived from sectional TPM_s extracted in **Step 1**. Then the synthesis of each section is dealt with separately. The corresponding Cumulative Probability Function is used to randomly generate velocity for the next time step. The detailed description of the synthesis process is presented by the authors in[23].

Vehicle model

In line with works of[24,25], the longitudinal vehicle model has been developed considering non-conservative forces related with aerodynamic drag (F_a) and rolling resistance (F_r). On the one hand, aerodynamic drag depends on the vehicle's frontal area A, the drag coefficient C_d, which is mainly function of the vehicle shape and surface roughness, the air density and the square of the vehicle speed (v):

$$F_a = \frac{1}{2} A C_d \rho v^2 \quad (3)$$

On the other hand, rolling resistance is represented by:

$$F_r = \mu m_v g \cos \beta \quad (4)$$

where μ is a friction coefficient, dependent on the tyre-tarmac contact, and therefore difficult to evaluate accurately, but generally assumed to be in the range of 0.01 to 0.015 for light duty vehicles. Regarding the rest of parameters, m_v is an equivalent vehicle mass accounting for the vehicle mass (m) but also for the inertia of the powertrain rotating parts, g is the gravity constant and β represents the road grade, that also leads to a force against the vehicle advance when it climbs (F_g) which expression is:

$$F_g = m_v g \sin \beta \quad (5)$$

Note that the energy required to overcome F_g when the vehicle is climbing can be theoretically recovered when going downhill to the initial position.

A force balance leads to the following ordinary differential equation:

$$F_t = m_v \dot{v} + F_a + F_r + F_g \quad (6)$$

which is the main equation of the vehicle longitudinal dynamics. The parameters in (3) are estimated from literature, (6) allows to calculate required engine speed and torque to fulfill the demanded vehicle speed profile.

Engine model

Within the elements of the vehicle powertrain, the engine is most complex due to the large amount of energy transformations and physical processes involved. This complexity makes it difficult to have real-time modelling capabilities for detailed engine physical models. In addition,

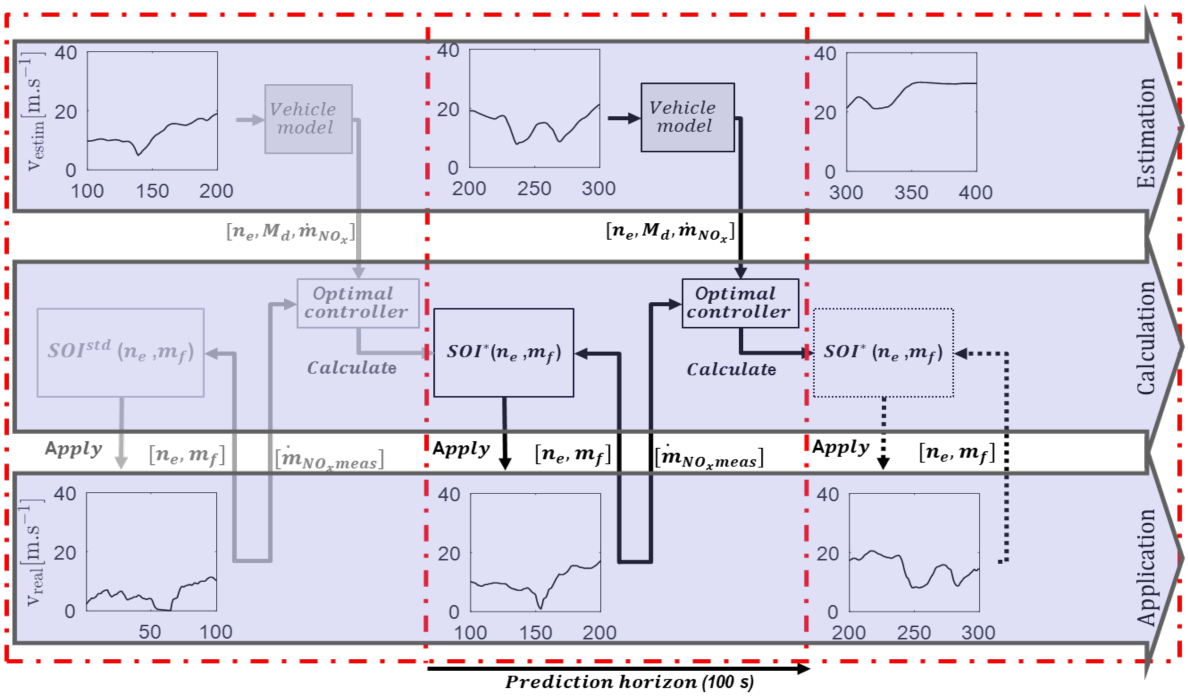

Figure 1. High level control schematic: Top row is vehicle speed prediction, middle row the calculation of optimal control and storing it as calibration maps and bottom row is the application of control to the real engine. Three columns represent time windows, where middle column represent the present time, left and right columns represent past and future time windows

the high number of states on high fidelity models make optimisation a very complex task since the computational burden of optimisation algorithms strongly depends on the number of states of the model. In this sense, a typical approach also shown by the authors in[26,27] is to assume that engine dynamics are not relevant or at least their characteristic times are much lower than those of the pedal actuation. In this sense, in the vehicle model, the engine torque, the fuel consumption and NO_x emissions are calculated by interpolation of experimental data as a function of engine speed (n_{eng}), load (M_d) and SOI.

Fuel consumption optimisation with constrained NO_x emissions

The inputs to the low level controller shown in Figure 2 are the estimated vehicle velocity $v(s)$, estimated engine speed n_e, engine torque M_d and dynamic NO_x emission limit ($\widehat{NO_x}^{dyn}$), which is updated after every PHW based on (7).

$$\widehat{\mathrm{NO_x}}^{\mathrm{dyn}} = \widehat{\mathrm{NO_x}} - \int_0^s \frac{\dot{\mathrm{m}}_{\mathrm{NO_x meas}}}{\mathrm{v_{meas}(s)}} \mathrm{ds} \tag{7}$$

where, $\widehat{NO_x}$ is the predefined emission limit for the entire trip, $\dot{m}_{NO_x meas}$ is the rate of NO_x emissions measured by the sensor, $v_{meas}(s)$ is the measured vehicle velocity and s is the distance travelled by the vehicle.

Within the controller there are quasi-steady engine model and an optimiser. The engine model performs online calculation of fuel consumption and NO_x emissions during the transient operations with different calibration maps in parallel. This is achieved by modelling engine as a set of maps as in (8)

$$\begin{gathered} \mathrm{m_f}(\mathrm{n_e}, \mathrm{M_d}, \mathrm{SOI}^{\alpha(k)}) \\ \mathrm{NO_x}(\mathrm{n_e}, \mathrm{M_d}, \mathrm{SOI}^{\alpha(k)}) \end{gathered} \tag{8}$$

The two outputs of the engine model are, m_f and NO_x emissions, which are fuelling rate and NO_x emissions depending on the calibration index k. The three inputs of the engine model are n_e, M_d and SOI. The base line calibration SOI^{std} is perturbed as shown in (9).

$$\begin{aligned} \mathrm{SOI}^{\alpha(k)} = \mathrm{SOI}^{\mathrm{std}} + \alpha_0(k) + \alpha_1(k) * \mathrm{n_e^{norm}} \\ + \alpha_2(k) * \mathrm{M_d^{norm}} \end{aligned} \tag{9}$$

where, α_0, α_1, $\alpha_2 \in [-1, 1]$, n_e^{norm}, M_d^{norm} are normalised engine speed and torque in euclidean space. Then, obtained calibrations are stored as vectors into a matrix A as in (10), where $\alpha(k)$ is a vector of the three coefficients of the k_{th} calibration.

$$A = \begin{bmatrix} \alpha(1) \\ \alpha(2) \\ \alpha(3) \\ . \\ . \\ \alpha(k) \end{bmatrix} ; \alpha = \begin{bmatrix} \alpha_0 & \alpha_1 & \alpha_2 \end{bmatrix} \tag{10}$$

It must also be noted that the lookup set must fullfil following conditions:

- They must lie within the feasible actuator boundary. In the current study, SOI was explored within [SOI^{std}-3,SOI^{std}+3] CAD, which is within the feasible boundary shown in Figure 3 for the engine under study.
- The engine must have senstivity to the changing calibrations within the look-up set.

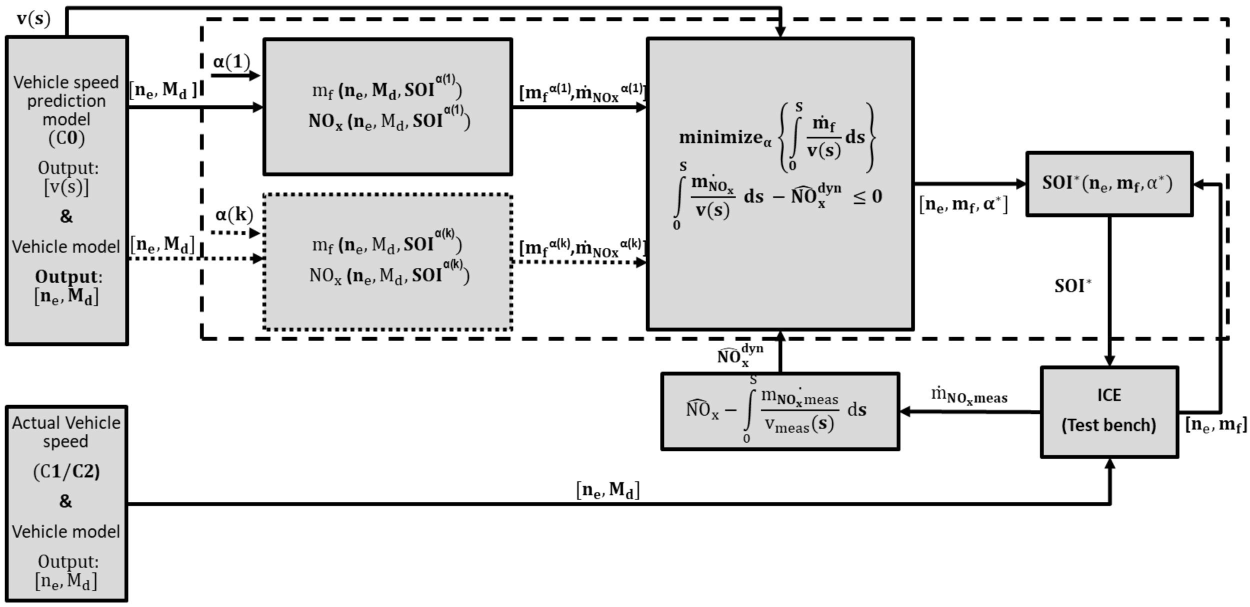

Figure 2. Low level controller schematic: Inside the dotted box are the engine model, a calculator and an adapted calibration map. Block in the top left the vehicle velocity prediction model and a vehicle model to obtain engine speed and torque from the predicted velocity. Block in the bottom left is the actual engine speed and torque measured on a real vehicle. ICE block is the engine test bench.

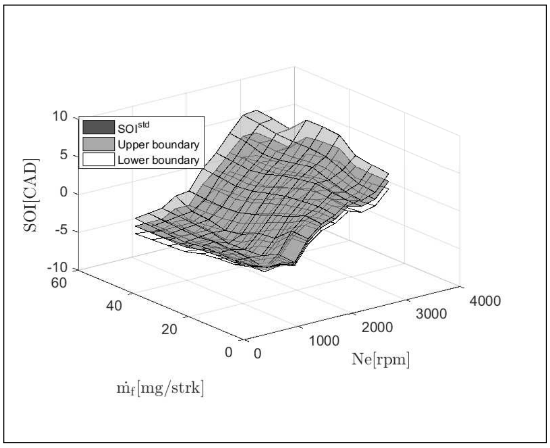

Figure 3. Standard SOI calibration map with the upper and lower boundary, within which the optimal maps have been explored

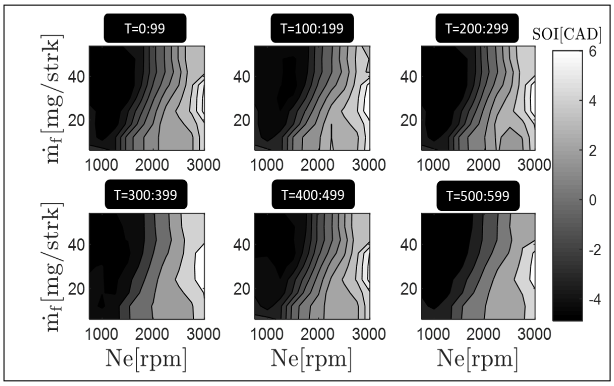

Figure 4. Representation of the adaptation of SOI calibration with time. Maps update at the end of the moving prediction horizon window of 100 s.

- Calibration maps must be smooth enough in order to fulfill conditions of drivability.

Finally, the controller selects an optimal calibration $\alpha(k)$ by solving the problem in (11), where fuel consumption is minimised for a given distance s while being within dynamic NO_x limits .

$$
\begin{gathered}
min_{\alpha(k)\in A} \int_0^s \frac{\dot{m f}}{v(s)} ds \\
\int_0^s \frac{\dot{m}_{NO_x}}{v(s)} ds - \widehat{\mathrm{NO}}_\mathrm{x}^{\mathrm{dyn}} \leq 0
\end{gathered} \tag{11}
$$

The components of α are discretised in 3 elements leading to 27 combinations which is the size of the lookup set. Figure 4, presents sequence of optimal calibration map adapting with time for the first 600 s of a real driving cycle. Naturally, the maps get updated in the map domain anticipated by the vehicle cycle predictor, which in the presented case is about 2000 rpm and low engine loads.

Experimental set up

The approach presented in this paper was tested on a Diesel engine with specifications as in (1) at CMT-Motores Termicos. The engine is coupled to an asynchronous Horiba DYNAS 3 dynos which is controlled with a Horiba SPARC through the PC interface Horiba STARS. The dyno is able to perform steady-state, transient and dynamic tests and in particular it is able to emulate the vehicle behaviour to carry out tests simulating real driving missions. An open Electronic Control Unit (ECU) was used to modify the SOI feedforward maps. With the modified SOI settings, the engine follows the desired torque profile acting on the engine throttle in closed loop with torque feedback. For which, a rapid prototyping system was connected via ECU ETK port allowing for sending and receiving the signals. This bypass

Stroke x Bore[mm]	84.8 x 75
Displacement[cc]	1498
Compression ratio	16:1
Number of Cyl.	Inline 4
Valves per Cyl.	4
Rated Torque	300Nm @ 1750rpm
Emission std.	Euro 6

Table 1. Engine specification

configuration is created using INTERCRIO and generated in the dSpace system. The hardware setup is composed of dSpace Microauto164 box II, ETAS 910 and an open ECU. The test-bench apparatus such as the fuel balance FQ2100 and the gas analyzer (GA) Horiba MEXA 7100 series are connected to the STARS interface. The NTC sensors and the Cambustion NDIR 500 gas analyzer are connected to the RPS dSpace by analogic signal, while the NO_x sensors are connected to the RPS dSpace by CAN protocol. For the concentrations measurements in the test bench, the Horiba MEXA 7100 DEGR GA is used to measure NO_x at one point of the exhaust line.

Results

In the current study three driving cycles are considered: The first cycle C0 is an estimated cycle, synthesized using the tool described in the previous section. The second and the third cycles - C1 and C2 respectively are recorded on a vehicle on the route under consideration. In Figure 5, the evolution of the vehicle speed is presented. The plots at the bottom shows the frequency of engine operations for the three cycles, it can be noticed that the aggressiveness of C0 is higher than C1 and less than C2. Using these three cycles, a case study was designed for the method validation. Three relevant scenarios are considered based on the driving dynamics of the predicted vehicle speed, driving dynamics of actual vehicle speed and limits over $\mathrm{NO_x}$ emissions.

- The first scenario $Scen1$ is when the actual driving cycle coincides with the estimated driving cycle.
- The second scenario $Scen2$ is when the aggressiveness of actual driving cycle is less than the estimated cycle.
- The third scenario $Scen3$ is when the aggressiveness of actual cycle is higher than the estimated cycle.

For each scenario, two cases $case1$ and $case2$ which are regarding the constraint on $\mathrm{NO_x}$ emission are presented, where $case1$ and $case2$ are with $\widehat{\mathrm{NO_x}}$ less than 0.2 g/km and 0.3 g/km respectively for the trip.

In Figures 6, 9 and 11, the result of the engine performance for the three scenarios are presented. The comparision is made with the engine performance using standard calibration (std_{cal}). It should be recalled that during the first 100 sec the controller applies standard calibration regardless of the $Scen$ or the $case$.

$Scen1$ In Figure 6 the estimation of driving cycle is perfect; therefore the estimation of emissions for PHW would be different from the actual emissions only due to the error in engine modelling, the difference due to driving uncertainity would be zero. In figure, 8 an enlarged view of 0-360 sec is presented. The emissions in g/km are very high

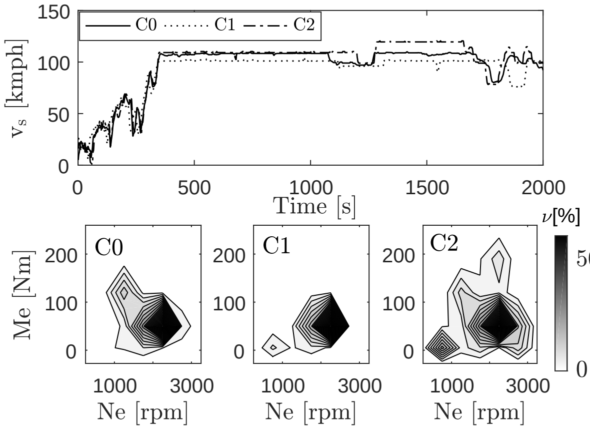

Figure 5. Predicted and measured vehicle speed on the route under consideration; frequency of engine operating points for the three cases velocity profiles

at the beginning of the cycle and therefore SOI is largely retarded for both the cases in order to reduce $\mathrm{NO_x}$ emissions. The difference in performance can be noticed with δm_f and $\delta\mathrm{NO_x}$ (defined in (12), as the percentage of cumulative deviation of fuel consumption or $\mathrm{NO_x}$ emissions for a $case$ and standard calibration). At the beginning of this phase of the cycle $\mathrm{NO_x}$ emissions are largely reduced; while at the end of this phase as the emissions are less than the limits, the controller emphasises on saving the fuel.

$$
\begin{aligned}
\delta m_f &= \frac{\int_0^s m_{f_{case1,2}} - \int_0^s m_{f_{std_{cal}}}}{\int_0^s m_{f_{std_{cal}}}} \times 100 \\
\delta \mathrm{NO_x} &= \frac{\int_0^s \mathrm{NO_{x_{case1,2}}} - \int_0^s \mathrm{NO_{x_{std_{cal}}}}}{\int_0^s \mathrm{NO_{x_{std_{cal}}}}} \times 100
\end{aligned} \tag{12}
$$

From 360-1800 sec vehicle speed is quite constant (representative of the highway driving) and only few transients appear due to the road slope effect, for $case1$ the SOI is retarded more than $case2$ to have lower $\mathrm{NO_x}$ emissions at the end of the cycle. For case2 the emissions are within the $\widehat{\mathrm{NO_x}}$ while for case1 emissions are 0.21g/km. For a lower emission constraint, adapting the calibration to the actual driving scenario allows to have 14 % reduction in emissions with a penalty of 1.3 % in fuel consumption. If the $\mathrm{NO_x}$ constraint is relaxed to 0.3 g/km and the calibration is adapted to the actual driving cycle, as in Figure 7, fuel consumption can be reduced by 0.9 % while limiting the $\mathrm{NO_x}$ emissions below 0.3g/km. It can be also observed that lower emission limit can be achieved with the calibration look-up set.

$Scen2$ In Figure 9, the actual driving cycle is less aggressive than the estimated driving cycle, therefore the estimation of emissions for PHW would be higher than the actual emissions. From 100-360 s, even though the vehicle is running at low velocity, the estimated emissions are more than actual and hence the SOI is retarded. For instance, during the second PHW, the estimation of emission is higher and therefore the control strategy is to minimise the emission as much as possible. At the beginning of third PHW the $\mathrm{NO_x}$ limit is corrected due to lower emission produced in second

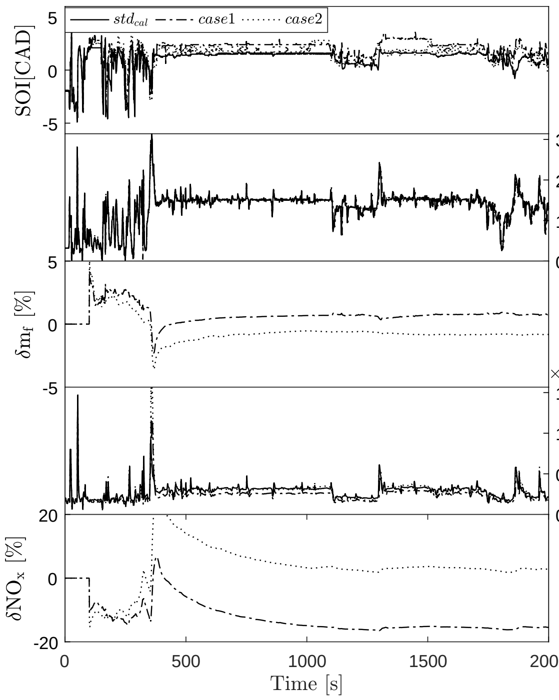

Figure 6. $Scen1$; Start-of-Injection; fuelling rate, difference of cumulative fuel mass, instanteneous NO_x emissions, difference of cumulative NO_x emissions

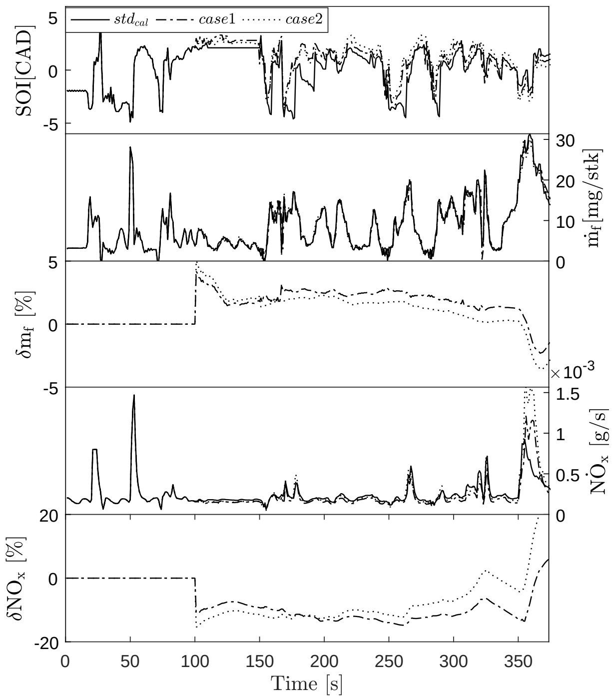

Figure 8. $Scen1, Zoom: 0 - 360sec$; Start-of-Injection; fuelling rate, difference of cumulative fuel mass, instanteneous NO_x emissions, difference of cumulative NO_x emissions

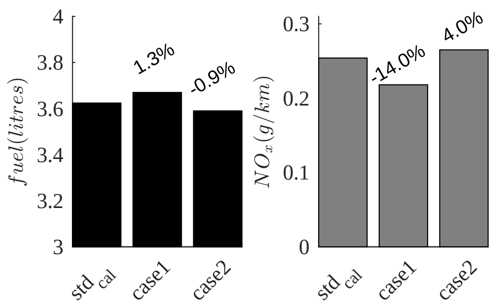

Figure 7. $Scen1$; Cumulative fuel consumption and NO_x emissions and their relative difference with standard calibration

PHW. The higher $\widehat{NO_x}^{dyn}$ limit, makes a calibraiton, favoring better fuel efficiency. Thereby, for $case1$, 5% reduction in emissions is possible while insignificant increase in fuel consumption as shown in Figure 10. In case 2, the fuel consumption can be improved upto 3.9 % while staying within the emission limits. Moreover, in both the cases the limits on NO_x emissions are fulfilled at the end of the cycle.

$Scen3$ In Figure 11, the actual driving cycle has higher aggressiveness than the estimated driving cycle. Accordingly, the estimation of emissions for PHW would be lower than the actual emissions, resulting in a strategy favouring NO_x reduction in the second PHW. Under-estimating the cycle aggressiveness leads to unfulfilled constraint in $case1$. In order to fullfill the NO_x limit, the SOI is largely retarded during the cycle. As presented in figure 12, emissions are reduced by 14% with a 1.1% penalty in fuel consumption for $case1$. In $case2$, it is possible to reach

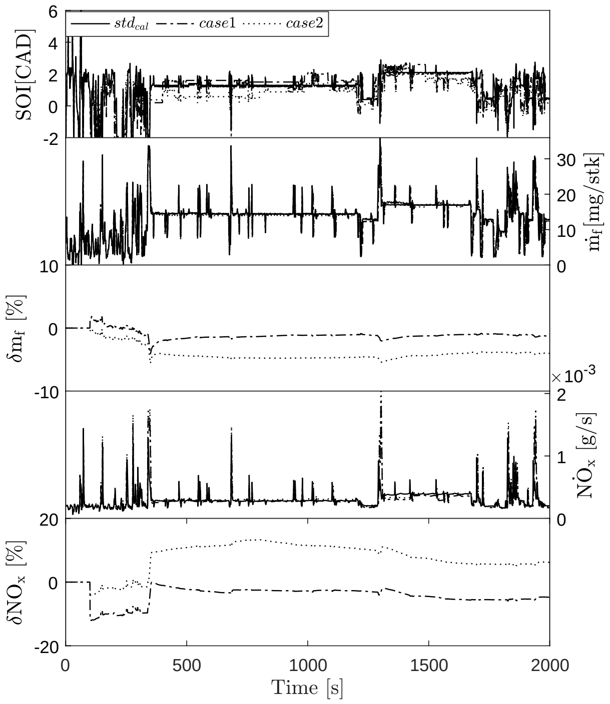

Figure 9. $Scen2$; Start-of-Injection; fuelling rate, difference of cumulative fuel mass, instanteneous NO_x emissions, difference of cumulative NO_x emissions

the emission target of 0.3 g/km, while further reducing fuel consumption by 0.8 %.

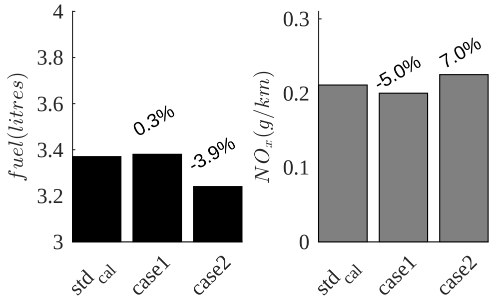

Figure 10. $Scen2$; Cumulative fuel consumption and $\mathrm{NO_x}$ emissions and their relative difference with standard calibration

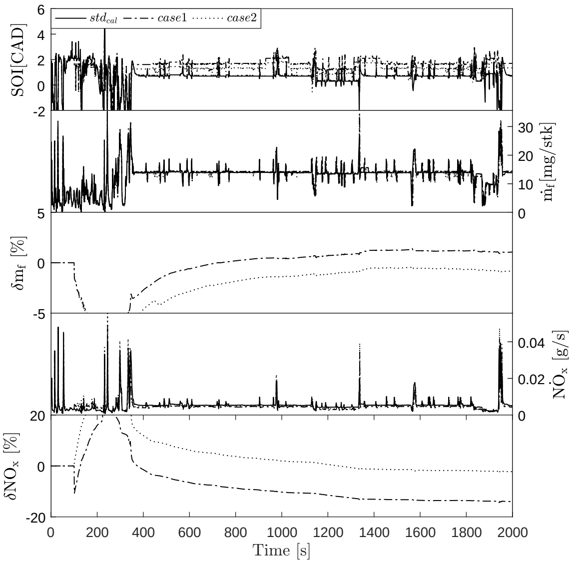

Figure 11. $Scen3$; Start-of-Injection; fuelling rate, difference of cumulative fuel mass, instanteneous NOx_x emissions, difference of cumulative NO_x emissions

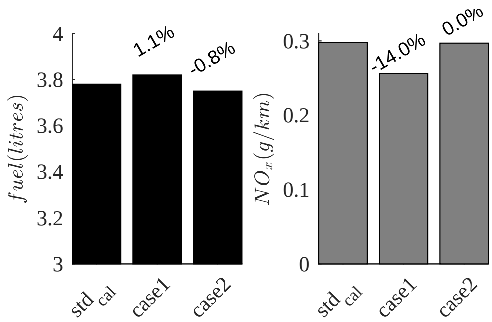

Figure 12. $Scen3$; Cumulative fuel consumption and $\mathrm{NO_x}$ emissions and their relative difference with standard calibration

The result can be summarised as:

- In scenarios 2, the constraints in both the cases are satisfied. Therefore considering a driving cycle with higher aggressiveness for calculating calibration is a preferred approach to fulfilling the $\mathrm{NO_x}$ constraint.
- In the first and third scenario, the constraint in $case1$ can not be fulfilled, this is because the range of the look-up set for SOI is limited to 6 CAD. Including more actuators and increasing their range will directly influence the range of achievable $\mathrm{NO_x}$ emissions at the expense of control complexity. In addition to the control actions taken, there is an impact of the driving condition itself on the fuel consumption and emissions. However with the developed methodology the emissions could be brought as close to the limit as possible by adaptation of the engine controls.

Summary and conclusions

The discrepancy in actual and declared Diesel engine emissions has raised a trend in applications which can optimise the engine performance during actual driving conditions. This paper has aimed to develop a pre-lookup based online adaptive calibration method to minimise fuel consumption with constrained $\mathrm{NO_x}$ emissions. In order to do that, three developments have been done: firstly, a vehicle and an engine model are developed to evaluate the engine perfomance in terms of fuel consumption and emission . Then, a vehicle speed prediction model is proposed which is based on the space dependent transition probability matrices obtained from the experimental data for a given route. Lastly, a controller is proposed which is capable of running in realtime and adapts the engine calibration based on the cumulative fuel consumption and real driving $\mathrm{NO_x}$ emission. Following the development of necessary tools, a case study was designed and tested on an engine testing set-up. The main contribution of the article according to the authors are as follows:

- The implementation of the proposed methodology shows that the $\mathrm{NO_x}$ emissions can be constrained in real driving condition. The developed method is a mid-way to optimal control methods, which are computationally expensive for real-time application and state-of-the-art method based on fixed calibration which do not take into account most of the real driving uncertainties.
- The study demonstrates a real-time capable application of the Markov based cycle prediction tool also shown by Lujan et al. in[28]. The proposed method takes the advantage of available information about the velocity profile on a given route.
- The study shows that aggressiveness is a critical parameter for evaluating real-time calibration of a Diesel engine. As the cycle prediction tool is efficiently able to capture the driving aggressiveness, with the proposed tool fuel consumption can be minimised upto 3 % while staying well within a predefined emission limit. Otherwise, the controller can not reduce the emissions below a certain level and then a driver advisory can be used to advise the driver about aggressiveness in order to fulfill emission targets.

Acknowledgements

The authors acknowledge the support of Spanish Ministrrio de Economia, Industria y Competitivad through project TRA2016-78717-R.

References

1. Vagnoni G, Eisenbarth M, Andert J et al. Smart rule-based diesel engine control strategies by means of predictive driving information. *International Journal of Engine Research* 2019; 20(10): 1047–1058. DOI:10.1177/1468087419835696.
2. Hooftman N, Messagie M, Van Mierlo J et al. A review of the european passenger car regulations–real driving emissions vs local air quality. *Renewable and Sustainable Energy Reviews* 2018; 86: 1–21.
3. Chen Y and Borken-Kleefeld J. Real-driving emissions from cars and light commercial vehicles–results from 13 years remote sensing at zurich/ch. *Atmospheric Environment* 2014; 88: 157–164.
4. Isermann R. *Engine Modeling and Control: Modeling and Electronic Management of Internal Combustion Engines*. Berlin, Germnay: Springer, 2014.
5. Millo F, Arya P and Mallamo F. Optimization of automotive diesel engine calibration using genetic algorithm techniques. *Energy* 2018; 158: 807–819. DOI:10.1016/j.energy.2018.06.044.
6. Lee TK and Filipi ZS. Synthesis of real-world driving cycles using stochastic process and statistical methodology. *International Journal of Vehicle Design* 2011; 57(1): 17. DOI:10.1504/ijvd.2011.043590.
7. Maroteaux F and Saad C. Combined mean value engine model and crank angle resolved in-cylinder modeling with nox emissions model for real-time diesel engine simulations at high engine speed. *Energy* 2015; 88: 515–527. DOI:10.1016/j.energy.2015.05.072.
8. Ozatay E, Onori S, Wollaeger J et al. Cloud-based velocity profile optimization for everyday driving: A dynamic-programming-based solution. *IEEE Transactions on Intelligent Transportation Systems* 2014; 15(6): 2491–2505.
9. Ozatay E, Ozguner U, Michelini J et al. Analytical solution to the minimum energy consumption based velocity profile optimization problem with variable road grade. *IFAC Proceedings Volumes* 2014; 47(3): 7541–7546.
10. Sciarretta A, De Nunzio G and Ojeda LL. Optimal ecodriving control: Energy-efficient driving of road vehicles as an optimal control problem. *IEEE Control Systems* 2015; 35(5): 71–90.
11. Zhijia Y, Richard S and Edward W. Online adjustment of start of injection and fuel rail pressure based on combustion process parameters of diesel engine. *SAE International* 2013; .
12. Jonas A, Oscar C and Lino G. Optimal contorl of diesel engines: Numerical methods, application, and experimental validation. *Hindawi Publishing corporation, Mathematical Problems in Engineering* 2014; .
13. Hellstrom E, Lee D, Jiang L et al. On-board calibration of spark timing by extremum seeking for flex-fuel engines. *IEEE Transactions on Control Systems Technology* 2013; 21(6): 2273–2279. DOI:10.1109/tcst.2012.2236093.
14. Corti E, Mancini G, Forte C et al. Automatic combustion phase calibration with extremum seeking approach. In *Volume 1: Large Bore Engines; Advanced Combustion; Emissions Control Systems ; Instrumentation, Controls, and Hybrids*. American Society of Mechanical Engineers. DOI:10.1115/icef2013-19132.
15. Popovic D, Jankovic M, Magner S et al. Extremum seeking methods for optimization of variable cam timing engine operation. *IEEE Transactions on Control Systems Technology* 2006; 14(3): 398–407. DOI:10.1109/tcst.2005.863660.
16. Quingyuan T, Prasad D, ying T et al. Online calibration of combustion phase in a diesel engine. *Contrl Theory and Technology* 2017; .
17. Andreas AM, Panos Y and Dennis NA. Online identification and stochastic control for autonomous internal combusiton engines. *Journal of Dynamic Systems, Measurement, and Control* 2010; .
18. Petri S, Vagnoni G, Aubeck F et al. Predictive engine and aftertreatment control concepts for a heavy-duty long-haul truck. In *27th Aachen Colloquium Automobile and Engine Technology 2018*.
19. Nishio Y and Shen T. Model predictive control with traffic information-based driver's torque demand prediction for diesel engines. *International Journal of Engine Research* 2019; : 146808741985167DOI:10.1177/1468087419851678.
20. Stephan Z, Jonas A, Christopher O et al. An equivalent emission minimization strategy for causal optimal control of diesel engines. *Energies* 2014; .
21. Gokul SS, Rohan CS, Chris M et al. Model predictive controller with average emissions constraints for diesel airpath. *Control Engineering Practice* 2019; .
22. Carlos G, Benjamin P, Pau B et al. Adaptive calibration for reduced fuel consumption and emissions. *Proceedings of the Institution of Mechanical Engineers, Part D: Journal of Automobile Engineering* March, 2016; .
23. Luján JM, Guardiola C, Pla B et al. Impact of driving dynamics in RDE test on NOx emissions dispersion. *Proceedings of the Institution of Mechanical Engineers, Part D: Journal of Automobile Engineering* 2019; : 095440701988158DOI:10.1177/0954407019881581.
24. Ozatay E, Ozguner U, Filev D et al. Analytical and numerical solutions for energy minimization of road vehicles with the existence of multiple traffic lights. In *Decision and Control (CDC), 2013 IEEE 52nd Annual Conference on*. IEEE, pp. 7137–7142.
25. Maamria D, Gillet K, Colin G et al. Optimal eco-driving for conventional vehicles: Simulation and experiment. *IFAC-PapersOnLine* 2017; 50(1): 12557–12562.
26. Krost P, Hübner W and Hasse C. A physical-based approach for modeling cycle-to-cycle variations within a zero-dimensional/one-dimensional simulation environment. *International Journal of Engine Research* 2017; 19(1): 55–66. DOI:10.1177/1468087417732882.
27. Guardiola C, Pla B, Pandey V et al. On the potential of traffic light information availability for reducing fuel consumption and NOx emissions of a diesel light-duty vehicle. *Proceedings of the Institution of Mechanical Engineers, Part D: Journal of Automobile Engineering* 2019; 234(4): 981–991. DOI:10.1177/0954407019867167.
28. Luján JM, Guardiola C, Pla B et al. Impact of driving dynamics in RDE test on NOx emissions dispersion. *Proceedings of the Institution of Mechanical Engineers, Part D: Journal of Automobile Engineering* 2019; : 095440701988158DOI:10.1177/0954407019881581.